International Journal of Modern Manufacturing Technologies
ISSN 2067–3604, Vol. XV, No. 3 / 2023
https://doi.org/ 10.54684/ijmmt.2023.15.3.60

DEVELOPMENT OF HEART-LIKE STRUCTURE EMPLOYING ADDITIVE MANUFACTURING TECHNOLOGIES

Nikolaos Kladovasilakis[1,2], Paschalis Charalampous [1], Ioannis Kostavelis[1,3], Konstantinos Petsios[4], George Sarris[5], Dimitrios Tzetzis[2], Dimitrios Tzovaras[1]

[1] Centre for Research and Technology Hellas – Information Technologies Institute (CERTH/ITI), Thessaloniki, 57001, Greece
[2] Digital Manufacturing and Materials Characterization Laboratory, School of Science and Technology, International Hellenic University, Thessaloniki, 57001, Greece
[3] Department of Supply Chain Management, School of Economics and Business Administration, International Hellenic University, 60100 Katerini, Greece
[4] Onassis Cardiac Surgery Center, Clinical Research Unit, Athens, 17674, Greece.
[5] 3DLife SA, Athens, 15125, Greece

Corresponding author: Dimitrios Tzetzis, d.tzetzis@ihu.edu.gr

Abstract: This study aims to present a workflow concerning the retrieval of a human heart's 3D model and its fabrication with heart-like materials producing a 3D printed replica. In detail, the 3D model of the examined heart was obtained by applying a 3D reconstruction methodology utilizing DICOM data derived from CT-scans. For the 3D printed heart-like material, the Material Jetting AM technique was employed due to its ability to fabricate 3D printed composite parts with variable properties. Several compositions for the print-out materials were examined, and the material with the appropriate mechanical behavior compared to the actual heart, i.e. RWT-ENT A50 composite, was utilized. The 3D printing process of the physical heart-like structure was performed with the highest accuracy. Finally, the 3D printed heart-like structure was evaluated in terms of dimensional accuracy and surface roughness achieving sufficient accuracy with mean absolute error of 1.05mm and mean surface roughness of 2.78μm.

Keywords: Additive manufacturing, Material Jetting, Heart-like structure, 3D Reconstruction, Cardiology.

1. INTRODUCTION

The extensive research and the rapid developments of Additive manufacturing (AM) technology in the recent years have led to its utilization as a fabrication technique in a plethora of industrial sectors, such as medical, biomechanical, automotive, etc. [1,2,3]. In particular, the employment of multi-material 3D printing techniques provides the ability to construct 3D models with tissue-like materials. Furthermore, the development of advanced 3D imaging and reconstruction algorithms support new technological tools for a wide range of applications in the medical sector. Some of these applications are innovative visualization techniques, educational purposes in medicine, medical and surgical training and further experimentation in organ's replicas [4].
In this context, in the last decade, numerous studies have investigated novel 3D imaging, reconstruction, and segmentation techniques in order to produce accurate digital 3D models, especially in cardiology due to the complexity and significance of the human heart and cardiovascular system [5,6]. More specifically, Byrne et al. [5] conducted a comprehensive review of the 3D imaging and reconstruction for the cardiovascular system, examining 136 published studies and concluding that there is a reliance on manual and semi-automated reconstruction and segmentation methods which demand a high level of expertise and a sufficient time commitment on the part of the user. It is worth mentioning studies like Jaros et al. [6], which developed an algorithm for automatic reconstruction and segmentation for medical imaging mainly focused on the 3D reconstruction of the heart and liver. Moreover, a patient-specific digital 3D model can be utilized for better visualization of the examined case, but also could be used for further analysis, such as Computational Fluid Mechanics (CFD) and Finite Element Analysis (FEA), in order to locate the system's defect, understand its nature and facilitate its resolve [7]. In detail, Schwarz et al. [7] published a review of modelling applications for a cardiovascular system utilizing 3D realistic models. In addition, increased scientific interest has gained the fabrication of 3D printed replicas for human organs in order to provide tangible patient-specific 3D models

constructed with tissue-like materials or color contours for an enhanced perception and visualization [8,9]. Taking into account these studies, it is derived that 3D printing with tissue-like materials can decrease the early-surgeon learning curve, enhance the surgeon's preparation for complex surgical operations as well as highlight the existing disease on the examined human tissue from further investigation.

In this context, the current article aims to present an automatic 3D reconstruction algorithm employed for heart modelling coupled with a detailed workflow for the production of a patient-specific 3D printed heart model constructed with heart-like materials. More specifically, the marching cubes methodology along with filtering algorithms were utilized for the automatic 3D reconstruction process. In addition, the innovative AM technique of multi-material jetting was applied in order to achieve a heart-like material in the produced 3D printed heart-like structure. The rest of the paper is organized as follows: Subsection 2.1 describes the automatic 3D reconstruction methodology of a human heart using the acquired data from CT-scans to accurately model the investigated heart. Subsection 2.2 is focused on the utilized materials and the applied AM technology. Subsection 2.3 analyses the experimental testing methodology along with the employed process for dimensional accuracy evaluation of the 3D printed component. Finally, Section 3 states the results for the available composite materials highlighting the composite material with behavior similar to the heart tissue/muscle. Moreover, in this section, the digital and the physical 3D models of the examined heart are presented coupled with an investigation of the dimensional accuracy of the printed heart via their comparison considering Surface Distance Maps (SDMs) and the 3D prints' surface roughness. Figure 1 depicts a detailed flowchart of the current research.

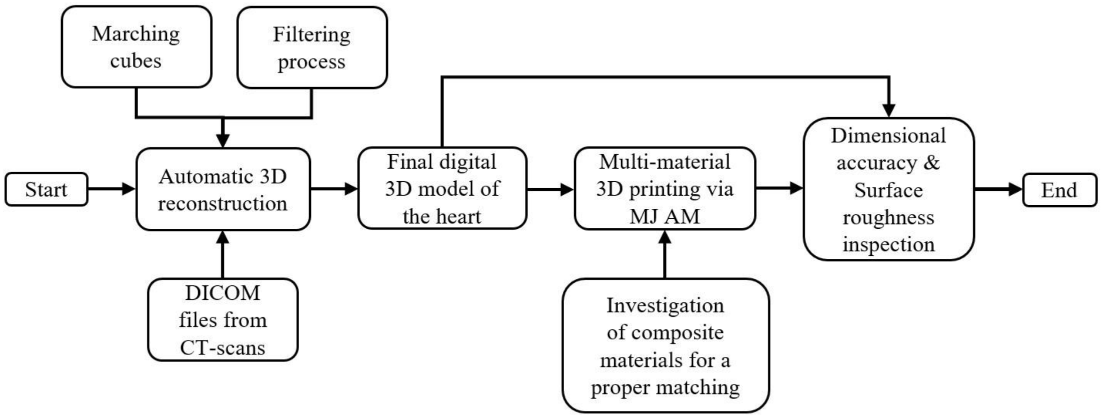

Fig. 1. Flowchart of the current research.

2. MATERIALS AND METHODS

2.1. 3D Reconstruction Methodology

The applied methodology of the present study is established with the automatic 3D reconstruction of a human's heart 3D model taking into account medical data. In particular, DICOM (Digital Imaging and Communications in Medicine) data that are derived from the CT scanning process are used as input to the developed algorithm in order to create the corresponding patient-specific heart's digital model. DICOM protocol is structured and standardized in a way that allows for interoperability between different medical imaging systems and equipment from different manufacturers. In addition, this type of data contains information about the image acquisition parameters, such as the number of slices, slice thickness, and slice spacing, which are essential for accurate image reconstruction [10]. One of the most popular approaches for 3D reconstruction tasks is the Marching Cubes algorithm which is a computer graphics technique utilized for creating 3D surfaces from a set of 3D data points, such as medical imaging data [11]. As is showed in Figure 2a, the Marching Cubes algorithm is based on the dividing a 3D space into a grid of cubes, where each of these cubes is analysed to determine which parts of the surface belong to the reconstructed 3D model. This is accomplished via the examination of the intensity values of the cube's corner points compared to a predefined threshold, visualizing that way the desired area of interest. Based on these values, the algorithm assigns a unique binary code to each cube, representing the location of the surface relative to the cube. In the next step, the proposed methodology generates a surface that passes through the appropriate edges of each examined cube, generating a complete 3D surface. Hereupon, the resulting surface is a mesh of triangles, which can be rendered using standard computer graphics techniques. In addition, several filtering algorithms can also be applied in order to filter out the outliers as well as the noise of the scene. The results of the employed method are demonstrated in Figure 2b, where the initial output of the marching cube algorithm is displayed in the left part (1) of Figure 2b. In the next two phases (2, 3), filtering approaches are utilized to remove large (2) and small parts (3) of the scene that are not directly attached to the examined heart. The final output of the employed methodology is illustrated in the right part (4) of Figure 2b, where smoothing of the 3D mesh as well as the manually trimming procedures of the area of interest were conducted in order to isolate the investigated heart.

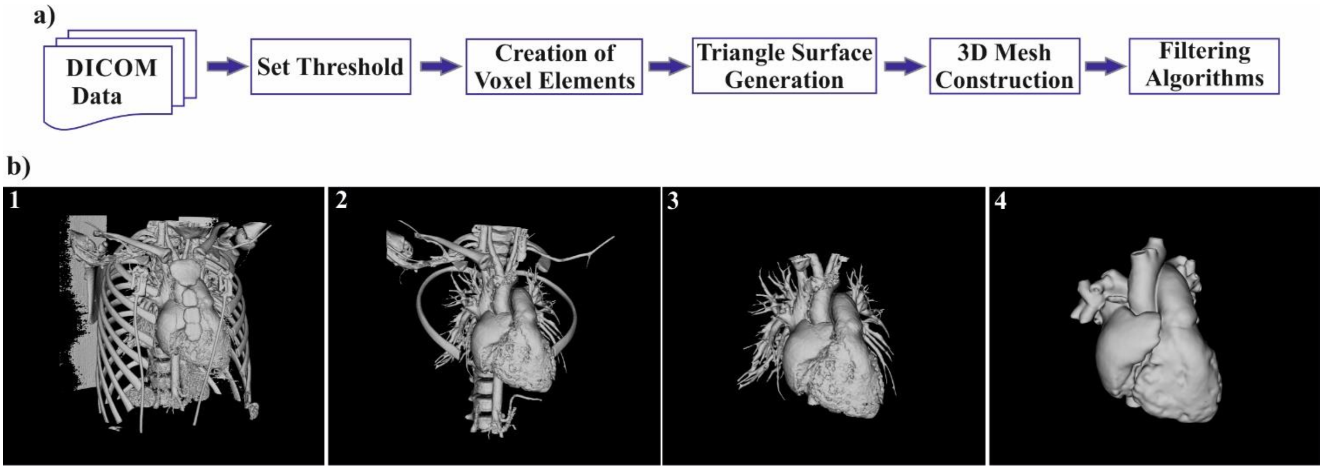

Fig. 2. a) Steps of the employed 3D reconstruction methodology, b) Results of the applied method on the examined human heart.

2.2. Materials and Additive Manufacturing

Prior to the 3D printing of the heart's model, it is essential to identify a construction material with properties similar to the heart tissue. Therefore, Material Jetting AM technology was utilized via the ProJet MJP 5600 3D Systems 3D™ printer. This process is based on the utilization of inkjet printing techniques in order to selectively deposit droplets through the printhead's jets and solidify them with UV lights creating that way a physical 3D object [12]. The particular 3D printer can perform a multi-material 3D printing process meaning a simultaneous 3D printing of two or more materials in the same layer. Moreover, it mixes two base materials in order to print composites with tailored properties. More specifically, for this study, ProJet MJP 5600™ utilized two base materials, the polycarbonate-like material with the commercial name VisiJet CR-CL 200™ as rigid material and the rubber-like material with the commercial name VisiJet CE-NT™ as elastomer material. The selection of these two base materials can potentially produce twelve different material compositions employing each time different fractions of each one. Taking into account that capability of the 3D printer, structures can be fabricated with a wide range of elasticity, namely from 0.35MPa (rubber-like) to 1750MPa (polycarbonate-like). Hereupon, in the context of this study, the properties of the heart tissue materials were investigated in the existing literature, and the five composites with the closest mechanical performance, according to the manufacturer, were 3D printed and tested in order to identify the one with the closest performance. The five selected composites have the following commercial names: RWT-ENT A80 RWT-ENT A70 RWT-ENT A60 RWT-ENTA50 and RWT-ENT A40, with the last three characters highlighting the mean value of the Shore A hardness. It is worth noting that the exact composition of each composite is not disclosed by the manufacturer. Regarding the 3D printing process, the XYZ printing orientation was utilized, according to the ASTM standardization [13], and a layer height of 13μm was selected in order to produce components with the maximum quality and dimensional accuracy.

2.3. Mechanic Testing and Evaluation

In this section, the employed evaluation techniques are presented with the first one is used to calculate the mechanical behavior of examined composites in order to choose the proper one. For this process, tensile and compression specimens were designed, manufactured via the MJP 3D printer, and tested according to international standardization [14,15], extracting that way the main mechanical properties, such as elastic modulus and ultimate tensile strength, coupled with the corresponding stress-strain diagrams. In particular, a universal testing machine, namely the Testometric M500-50AT, was employed equipped with a 500N load cell at room temperature. It is worth mentioning that all tests were conducted with a strain rate of 5mm/min [16]. Finally, each test was performed at least three times in order to extract reliable and accurate results.

The dimensional accuracy inspection of the 3D printed heart-like structure compared to its digitally reconstructed 3D model was performed utilizing the Artec Eva™ 3D scanner. Artec Eva™ is a portable structured-light 3D scanner with an accuracy of up to 0.1mm for small to medium size objects. In order to maximize the precision, the high-definition data acquisition was selected with up to 18 million points per second and a capturing speed was set at 16 frames per second. In the next step, the captured geometry of the 3D printed heart-like structure was compared with the heart's 3D model by applying the SDM methodology and evaluating the Mean Absolute Error (MAE). It is worth noting that this analysis was conducted on the Artec Studio™ software. In addition, surface roughness evaluation were performed utilizing multi-focus imaging employing the digital microscope Leica DMS 1000 and the software of MountainsLab®. Leica DMS 1000 had a plan- apochromatic objective achieving magnification up to 300×, capturing high- resolution images and conducting dimensional measurements. This equipment combined with the MountainsLab® software, exploited the captured multi-focus images and evaluated the 3D printed surface roughness with an accuracy of ±1μm.

3. RESULTS AND DISCUSSION

3.1. Print-out Materials Evaluation

The objective of the experimental evaluation of the selected composites is to identify the composite with similar mechanical performance to the actual heart muscle. Through the experimental tests that were previously discussed, the corresponding stress-strain diagrams for each material were extracted, as it is depicted in Figure 3. Moreover, the tensile stress-strain curves were magnified in the superimposed image for better understanding. As it was expected, intense elastomeric behaviors were observed for all examined materials, especially regarding the compression curves. Furthermore, the acquired tensile data shows that the stiffer materials had a better mechanical performance. However, all of the examined composite materials withstood extensive plastic strains with 90% of the strain derived from the plastic section both for compression and the tensile experiments. It is worth mentioning that during compression testing, the received stresses monotonically increase with higher slopes for the composite materials with stiffer behavior.

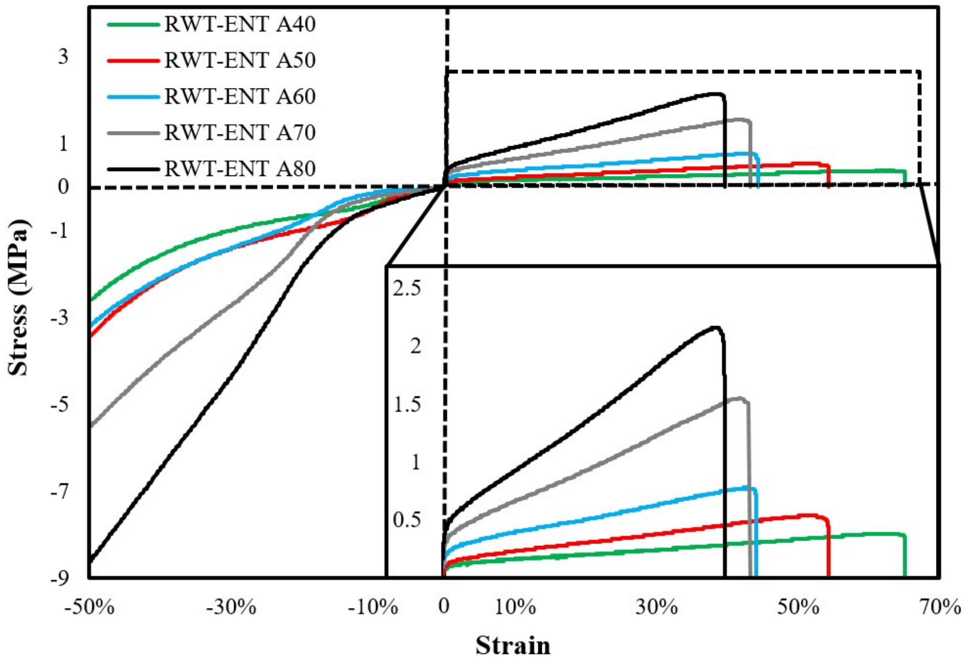

Fig. 3. Stress-strain diagrams of the examined composites for tensile and compression loading.

Table 1. Main properties of the examined composites compared to the heart tissue material [17,18].

Materials	Elastic modulus (MPa)	UTS (MPa)	Elongation at break (%)
Heart tissue	2.840	0.19	-
RWT-ENT A40	2.024	0.383	65.11%
RWT-ENT A50	3.562	0.539	54.31%
RWT-ENT A60	6.118	0.781	44.21%
RWT-ENT A70	10.51	1.552	43.20%
RWT-ENT A80	15.63	2.161	39.74%

Table 1 lists the main mechanical properties for each examined composite material, namely the elastic modulus, the ultimate peak strength (UTS), and the elongation at break, coupled with the passive mechanical properties of heart tissue/muscle. It is worth mentioning that the values of the mechanical properties for the heart tissue/muscle are different depending on the heart's region and the operation condition (systolic and diastolic). Thus, in the table below, indicative values are listed derived from passive testing on heart muscles from the existing literature [17,18]. The attained results show that the examined composites experienced high plastic strain with elongation at break from 39.74% to 65.1%. Moreover, the strength of the materials was proportional to their stiffness with the highest strength observed for the stiffest material, i.e. RWT-ENT A80. On the other, RWT-ENT A40 revealed the lowest elastic modulus with the lowest UTS at 0.383. Analyzing these results, the RWT-ENT A50 composite material presented the closest mechanical response to the heart tissue material in terms of elasticity, which is the most crucial property for material imitation in order to reveal similar elastic and plastic strains during the same loads. Therefore, the RWT-ENT A50 composite material was utilized as construction material for the 3D printing of the heart-like structure.

3.2. Digital and Physical 3D Model Evaluation

Considering the automatic 3D reconstruction process for the inspected human heart that was presented in the previous section, a patient-specific digital 3D model is derived, as it is portrayed in Figure 4a. The digital model was extracted in .STL mesh file format consisted of 1,490,572 facets and 4,471,716 vertices in order to accurately depict the heart's geometry. The external dimensions of the heart model were 109.38mm x 98.35mm x 143.06mm. Moreover, Figure 4b illustrates the 3D printed model of the heart-like material constructed with the RWT-ENT A50 composite material using the MJP 5600 3D printer. The 3D printed parts were additively manufactured without any visible defect revealing sufficient structural integrity and extensive elasticity.

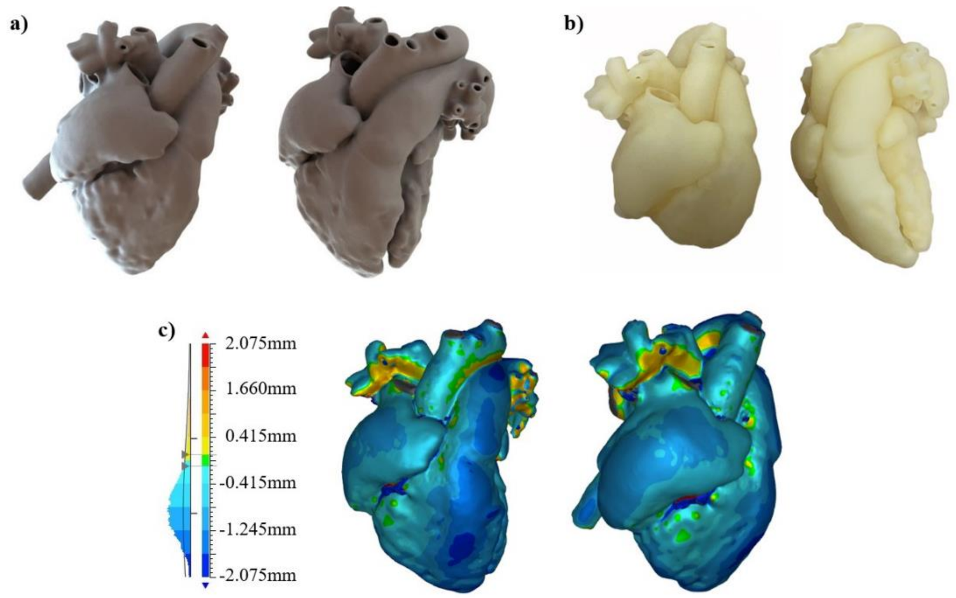

Fig. 4. a) Digital 3D model of the examined heart, b) 3D printed heart-like structure constructed with the RWT-ENT A50 composite, c) Surface distance maps for the reconstructed and the 3D printed model.

Furthermore, the 3D printed heart-like structures possessed a matte amber-like color facilitating the 3D scanning procedure. Concerning the 3D scanning process, five individual scanning procedures were conducted with an average of 1.52 million polygons each. Registration, outlier removal, alignment, and fusion algorithms were applied in order to combine these scans extracting that way a high-quality and accurate 3D model. In the next step, the dimensional accuracy was conducted via the SDM of the reconstructed 3D model and the scanned heart, as it is presented in Figure 4c. The outcome of the inspection process demonstrates that the 3D printed heart-like structure was slightly smaller compared to the digital one, due to the shrinkage effect that occurred during the photopolymerization process. The majority of the deviations ranged between - 1.66mm to - 0.415mm, some of them caused by 3D printing and 3D scanning inaccuracies. In addition, the MAE was calculated at 1.05mm showing a sufficient agreement between the 3D printed heart and the digital one, taking into account the elastomeric nature (easily deformable) of the construction material. The final evaluation process was the measurement of surface roughness on the 3D printed heart model. Surface roughness combined with the elasticity of the structure determine the compatibility and assembly configuration of the potential heart valves and stents. The 3D printed surfaces revealed low surface roughness with mean surface roughness (S_a) at 2.78μm and root mean square of surface roughness (S_q) at 3.64μm. Figure 5a shows an indicative surface map of a specific region of the 3D printed model, as it is obvious the examined surface is sufficiently smooth without peaks and pits. Furthermore, Figure 5b illustrates an indicative diagram of the surface roughness profile on a XY plane for the highlighted line of Figure 5a. It is noteworthy that for the measurement of surface roughness, multiple random regions of the 3D model heart model were examined in order to extract accurate and reliable results.

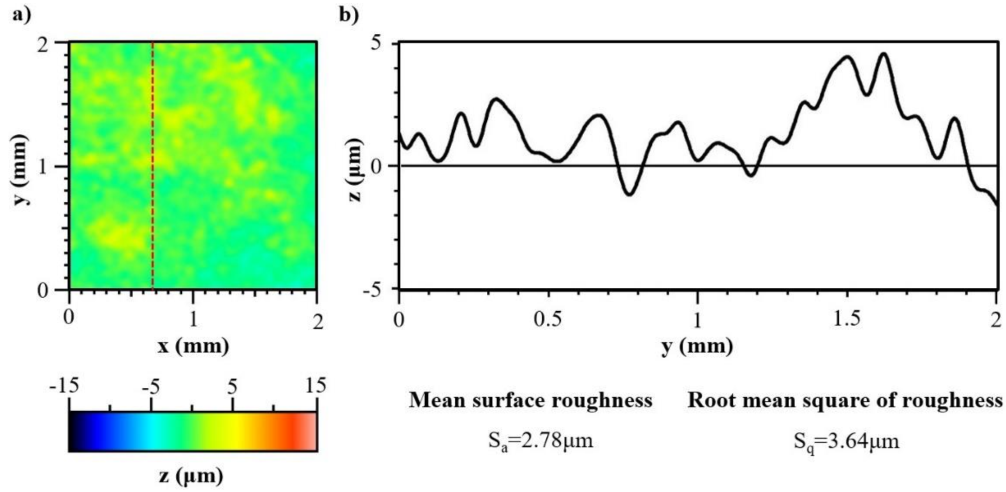

Fig. 5. a) Indicative roughness surface map of the 3D printed model, b) Indicative roughness of the model in XY plane.

4. CONCLUSIONS

In the current study, a detailed workflow for the retrieval of a human heart's 3D model and for the fabrication of a patient-specific 3D printed replica with heart-like materials and high fidelity was presented. More specifically, an automatic 3D reconstruction methodology was developed in order to generate a high-quality and accurate digital 3D model. Then, a material characterization process was performed between five different composite materials, compatible with the utilized multi-material AM equipment, identifying the composite material with the closest mechanical behavior to the heart tissue/muscle, where the RWT-ENT A50 material presented the closest mechanical performance in terms of elasticity. Therefore, the heart-like structure was fabricated utilizing this composite material and the material jetting AM process via the ProJet MJP 5600 3D printer. The produced 3D printed heart-like structure was manufactured without any visible defect and had sufficient structural integrity and extensive elasticity. The next step was the investigation of the printed heart dimensional accuracy through the employment of SDMs and the calculation of MAE between the reconstructed 3D digital model and the 3D printed model along with the measurement of surface roughness for the 3D printed model. The results of the dimensional accuracy analysis revealed that the 3D printed part was slightly smaller, mainly due to the shrinkage effect of the photopolymerization process and the MAE was calculated at 1.05mm. This value is relatively low considering the elastomeric nature of the construction material. Moreover, the 3D printed heart-like structure showed high surface quality with a mean surface roughness of 2.87μm. In future studies, further visualization processes, such as VR and AR, can also be integrated by exploiting the 3D reconstruction algorithm and enhancing the existing visualization experience. Finally, the developed 3D printed models can be combined with other tissue-like structures in order to assemble a high-quality dummy for surgical training on patient-specific cases.

Funding: This paper has received no external funding.

Acknowledgments: We acknowledge the support of this work by project 3D4KARDIA (project name 3D4KARDIA, project code: T2EDK - 04012), co-financed by the European Union and Greek national funds through the Operational Program Competitiveness, Entrepreneurship, and Innovation, under the call RESEARCH – CREATE – INNOVATE.

REFERENCES

1. Kladovasilakis, N., Kostavelis, I., Sideridis, P., Koltzi, E., Piliounis, K., Tzetzis, D., Tzovaras, D., (2023) *A Novel Soft Robotic Exoskeleton System for Hand Rehabilitation and Assistance Purposes*, Appl. Sci. 2023, 13, 553, https://doi.org/10.3390/app13010553.

2. Kladovasilakis, N., Charalampous, P., Boumpakis, A., Kontodina, T., Tsongas, K., Tzetzis, D., Kostavelis, I.; Givissis, P., Tzovaras, D., (2023) *Development of Biodegradable Customized Tibial Scaffold with Advanced Architected Materials Utilizing Additive Manufacturing*, Journal of the Mechanical Behavior of Biomedical Materials, http://dx.doi.org/10.2139/ssrn.4354973.
3. Kladovasilakis, N., Kontodina, T., Charalampous, P., Kostavelis, I., Tzetzis, D., Tzovaras, D., (2020) *A case study on 3D scanning, digital reparation and rapid metal additive manufacturing of a centrifugal impeller.* In Proceedings of the 24th Innovative Manufacturing Engineering and Energy International Conference (IManEE), Athens, Greece, 14–15 December 2020; 1037, 12-18. https://dx.doi.org/10.1088/1757-899X/1037/1/012018.
4. Farooqi, K., Cooper, C., Chelliah, A., Saeed, O., Chai, P.J., Jambawalikar, S.R., Lipson, H., Bacha, E.A. Andrew J. Einstein, A.J., Jorde, U.P., (2019) *3D Printing and Heart Failure*. J Am Coll Cardiol HF, 7 (2), 132–142. https://doi.org/10.1016/j.jchf.2018.09.011.
5. Byrne, N., Forte, V.M., Tandon, A., Valverde, I., Hussain, T., (2016) *A systematic review of image segmentation methodology, used in the additive manufacture of patient-specific 3D printed models of the cardiovascular system.* JRSM Cardiovasc Dis., 29 (5), https://doi.org/10.1177/2048004016645467.
6. Jaroš, M., Strakoš, P., Karásek, T., Říha, L., Vašatová, A., Jarošová, M., Kozubek, T., (2017) *Implementation of K-means segmentation algorithm on Intel Xeon Phi and GPU: Application in medical imaging*, Advances in Engineering Software, 103, 21-28, https://doi.org/10.1016/j.advengsoft.2016.05.008.
7. Schwarz, E.L., Pegolotti, L., Pfaller, M.R., Marsden, A.L., (2023) *Beyond CFD: Emerging methodologies for predictive simulation in cardiovascular health and disease*, Biophysics Rev., 4, 011301, *https://doi.org/10.1063/5.0109400*.
8. Wang, D., Qian, Z., Vukicevic, M., Engelhardt, S., Kheradvar, A., Zhang, C., Little, S.H., Verjans, J., Comaniciu, D., O’Neill, W.W., Vannan, M.A., (2021) *3D Printing, Computational Modeling, and Artificial Intelligence for Structural Heart Disease.* J Am Coll Cardiol Img. 14 (1), 41–60, https://doi.org/10.1016/j.jcmg.2019.12.022.
9. Qian, Z., Wang, K., Liu, S., Zhou, X., Rajagopal, V., Meduri, C., Kauten, J.R., Chang, Y.H., Wu, C., Zhang, C., Wang, B., Vannan, M., (2017) *Quantitative Prediction of Paravalvular Leak in Transcatheter Aortic Valve Replacement Based on Tissue-Mimicking 3D Printing*. J Am Coll Cardiol Img. 2017 Jul, 10 (7) 719–731. https://doi.org/10.1016/j.jcmg.2017.04.005.
10. Osti, F., Santi, GM., Neri, M., Liverani, A., Frizziero, L., Stilli, S., Maredi, E., Zarantonello, P., Gallone, G., Stallone, S., Trisolino, G., (2019) *CT Conversion Workflow for Intraoperative Usage of Bony Models: From DICOM Data to 3D Printed Models*. Applied Sciences., 9(4):708. https://doi.org/10.3390/app9040708
11. Nguyen, V.S., Tran. M.H., Quang Vu, H.M. (2016) *A Research on 3D Model Construction from 2D DICOM*. International Conference on Advanced Computing and Applications (ACOMP), Vietnam, 158-163, https://doi.org/10.1109/acomp.2016.031.
12. Kladovasilakis, N., Charalampous, P., Tsongas, K., Kostavelis, I., Tzetzis, D., Tzovaras, D., (2021) *Experimental and Computational Investigation of Lattice Sandwich Structures Constructed by Additive Manufacturing Technologies*. J.Manuf. Mater. Process., 5, 95. https://doi.org/10.3390/jmmp5030095.
13. ASTM ISO/ASTM52921-13; *Standard Terminology for Additive Manufacturing-Coordinate Systems and Test Methodologies*. ASTM International: West Conshohocken, PA, USA, 2013. https://doi.org/10.1520/ISOASTM52921-13R19.
14. BS EN ISO 527, *Plastics – Determination of tensile properties*, 2019, https://doi.org/10.3403/BSENISO527.
15. ISO 604, *Plastics – Determination of compressive properties*, 2002, https://dx.doi.org/10.31030/9515267.
16. Siviour, C.R.; Jordan, J.L., (2016) *High strain rate mechanics of polymers: a review*. J Dynamic behavior mater, 2, 15–32. https://doi.org/10.1007/s40870-016-0052-8.
17. Langewouters, G.J., Wesseling, K.H., Goedhard, W.J., (1984) *The static elastic properties of 45 human thoracic and 20 abdominal aortas in vitro and the parameters of a new model*, J Biomech, 17(6): 425-435. https://doi.org/10.1016/0021-9290(84)90034-4.
18. Bank, A.J., Wang, H., Holte, J.E., Mullen, K., Shammas, R., Kubo, S.H., (1996) *Contribution of Collagen, Elastin, and Smooth Muscle to In Vivo Human Brachial Artery Wall Stress and Elastic Modulus,* Circulation, 94, 3263-3270. https://doi.org/10.1161/01.CIR.94.12.3263.

Received: May 20, 2023 / Accepted: December 15, 2023 / Paper available online: December 20, 2023 © International Journal of Modern Manufacturing Technologies